Supporting Information

Position and Frequency Control of Strain-Induced Quantum Emitters in WSe_2 Monolayers

Hyoju Kim,[†,§] *Jong Sung Moon,*[†,§] *Gichang Noh,*[‡] *Jieun Lee,*[‡] *and Je-Hyung Kim*[*,†]

[†]School of Nature Science, Department of Physics, Ulsan National Institute of Science and Technology (UNIST), Ulsan 44919, Republic of Korea

[‡]Department of Physics and Department of Energy Systems Research, Ajou University, Suwon 16499, Korea

S1. Fabrication processes

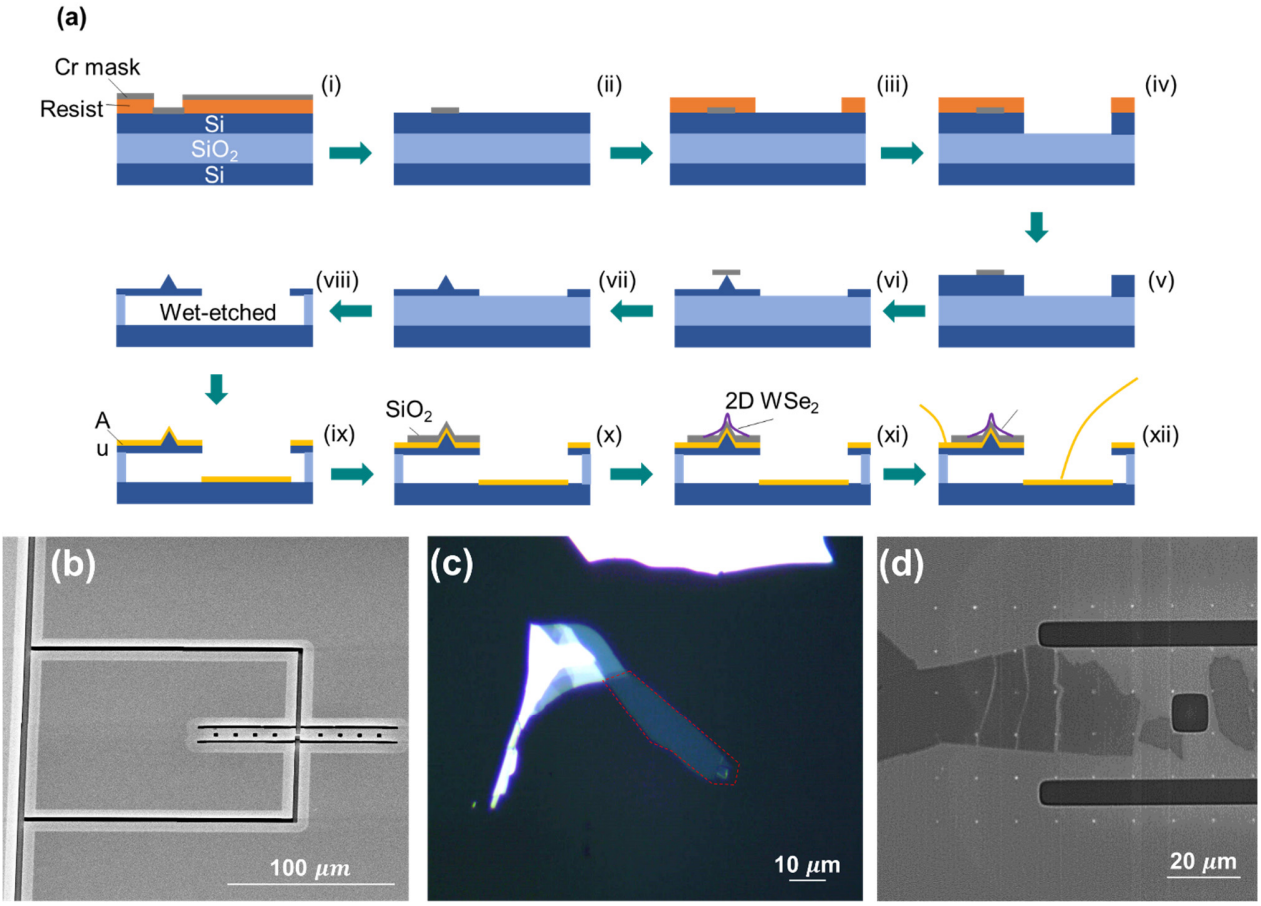

Figure S1. (a) Schematics of the sample preparation process, (b) Scanning electron microscopy image of the fabricated microcantilever device. (c) Optical image of the mechanically exfoliated WSe_2 few layers on a PDMS film. Red dash line denotes a monolayer region. (d) Scanning electron microscopy image of the integrated WSe_2 monolayer on the nanopatterned actuator.

Figure S1a shows a schematic of the fabrication processes for the device. We first form 300 nm x 300 nm nanopattern arrays using electron-beam lithography followed by a metal lift-off process. Then, we pattern the actuator device consisting of two connected cantilevers, described in Figure 1, using the second electron beam lithography. Inductively coupled plasma-reactive ion etching (ICP-RIE) process defines the actuator device. After the removal of the patterned resists, the second ICP-RIE forms the pyramidal-shaped nanopatterns shown in Figure 2c. The selective wet etching process of a SiO_2 sacrificial layer forms an air-suspended actuator device. For defining electrodes, we deposit an Au(30 nm)/Cr(5 nm) metal layer that forms the top and bottom electrodes for applying a voltage to the actuator. To prevent emission quenching by the metal layer, we also

deposit a 30 nm thick SiO_2 layer. Figure S1b shows a scanning electron microscopy image of the fabricated device. A few layered WSe_2 is prepared by mechanical exfoliation from a commercially available bulk WSe_2 (Figure S1c). The exfoliated WSe_2 layers are transferred to the actuator device using a direct polymer transfer method with a PDMS stamp. Figure S1d shows the integrated WSe_2 on the nanopatterned microcantilever. Finally, the electrodes of the sample are connected to the sample holder with a wire bonding technique.

S2. Simulation of reflectance from Au mirror

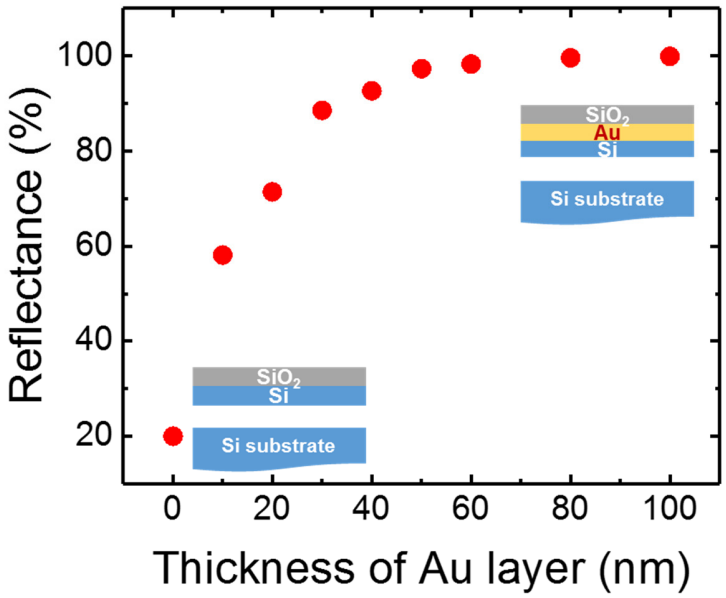

Figure S2. Simulation data of the reflectance of the Au coated micro-cantilever with different thickness of the Au layer.

When we fabricate the actuator device, we deposit a 40 nm thickness Au layer on the micro-cantilever for the top electrodes beneath the WSe_2 monolayer with a 30 nm thickness of SiO_2 for separation. This Au layer can also act as a good mirror, which efficiently reflects the downward quantum emission from the WSe_2 monolayer. To estimate the reflector effect, we use the finite-difference time-domain simulation. Figure S2 presents the simulated reflectance of the Au layer with different thickness at the wavelength of WSe_2 quantum emitters. Without the Au layer, the structure shows about 20% reflection from the Si cantilever and bottom substrate, while the reflectance significantly increases with the thickness of the Au layer. At the experimentally deposited 40 nm thick Au layer, we expect that 93 % of downward emission is reflected upward. Therefore, the Au layer can play as a good reflector for the integrated WSe_2 monolayers as well as the electrode.

S3. Intensity behavior on power variations

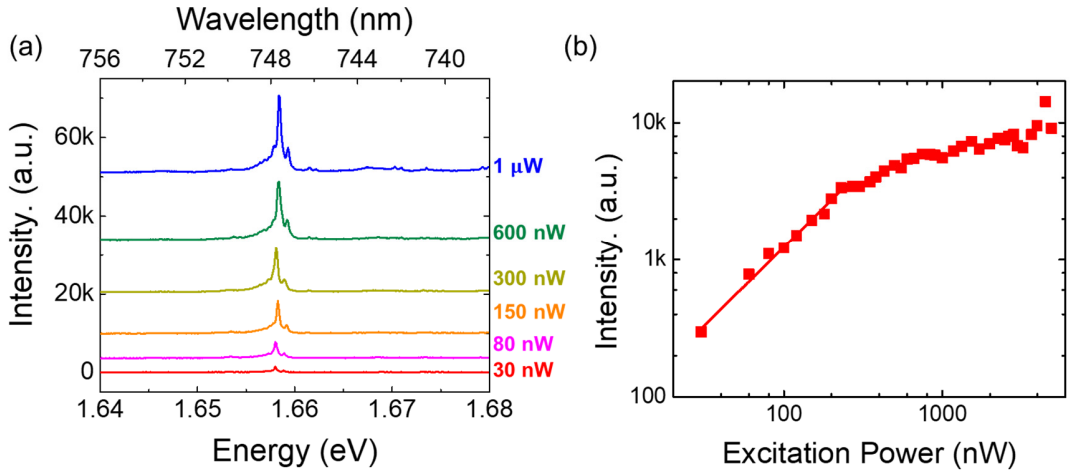

Figure S3. (a) Photoluminescence spectra of the WSe_2 monolayer on a nanopyramid with different excitation laser powers. (b) Intensity plot with the excitation power. Red squares show the measured intensity, and a red line presents a fitted line.

Figure S3a and S3b exhibit the photoluminescence spectrum and the integrated intensity with an excitation laser power. In Fig. S3b, we fit the data with the function $I = A + BP^{\alpha}$, where the fitting parameters A and B are background signals and proportional constant, respectively. The parameter α is related to the possible exciton multicomplex. In our experiment, α is 1.14, which indicates that the peak in the spectrum corresponds to a single exciton. Also, the peak shows the saturation behavior at around 407 nW, supporting that the peak originated from single localized exciton.

S4. Comparison of simulation and experimental result of cantilever deflections

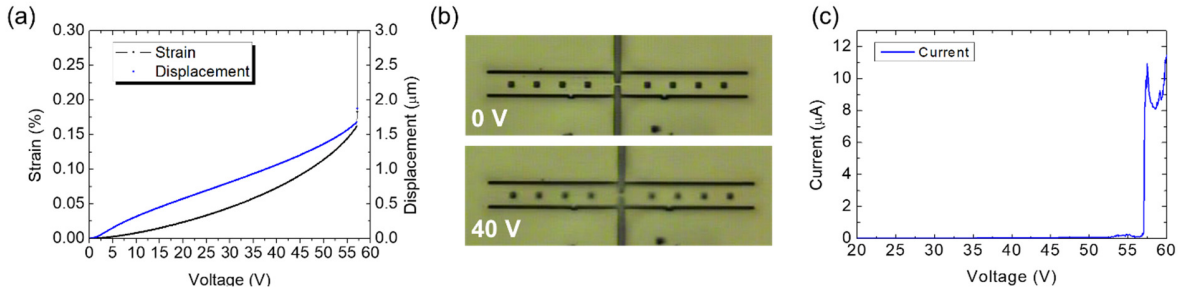

Figure S4. (a) Simulation results of the displacement and strain of the designed cantilever. (b) Optical images of the microcantilever at dc voltage of 0 V (upper) and 40 V (lower). (c) Experimental data of I-V curve for the fabricated cantilever.

We simulate the microcantilever deflection with an electrostatic force to identify the pull-in voltage ($V_{pull\text{-}in}$), which determines a maximum performance range for the frequency tuning in the main text. Using the finite element method, we model the microcantilever consisting of two cantilevers connected by a tether with the same dimensions as the fabricated cantilever. The applied material on the cantilever is silicon that has Young's modulus of 170 GPa and Poisson ratio of 0.28. Figure S4a plots the resulted displacement and strain of the cantilever with the applied voltage. The displacement (strain) was recorded at the center tether (the top of the clamped edge) of the device. In the simulation, we determine the $V_{pull\text{-}in}$ where the simulation starts to diverge. Near the $V_{pull\text{-}in}$ of about 55~60 V, the strain is estimated by 0.16 %, as shown in Figure S4a.

To experimentally identify the $V_{pull\text{-}in}$ of the fabricated device, we apply a dc voltage on the microcantilever and monitor an I-V curve. With increasing the voltage, the center part of the cantilever goes out of focus due to the deflection of the cantilever (Fig. S4b). In the I-V curve, we observe a sudden increase at the current above 55 V, indicating that the cantilever touched the bottom silicon substrate. The measured $V_{pull\text{-}in}$ is well matched to the simulated $V_{pull\text{-}in}$.

S5. Timing jitter on 2D WSe_2 single photon source

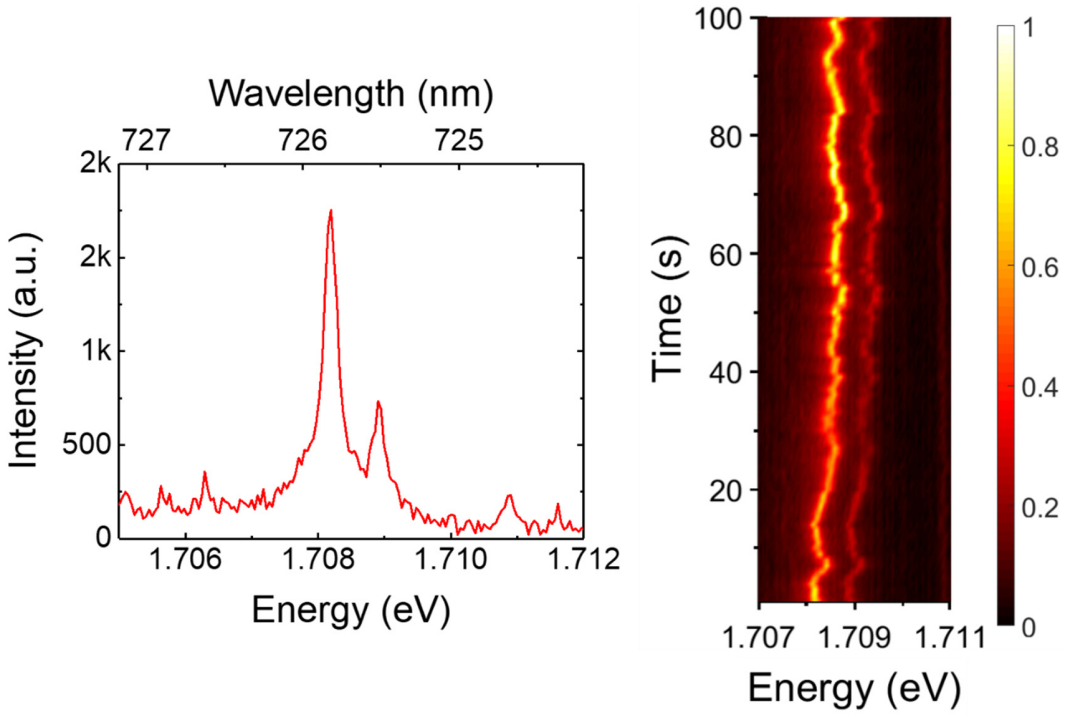

Figure S5. (Left) The spectrum of measured spectral jitter. (Right) Observation of spectral jitter on time to 100 seconds. The time-correlated doublet represents that they are fine structures of the single exciton.